Semi-Inclusive Λ electroproduction in the Target Fragmentation Region

A 12 GeV Proposal to Jefferson Lab PAC 42

S. Anefalos Pereira, G. Angelini, E. De Sanctis, D. Hasch, V. Lucherini, M. Mirazita[†,*], R. Montgomery, S. Pisano
Istituto Nazionale di Fisica Nucleare, Laboratori Nazionali di Frascati, P.O. 13, 00044 Frascati, Italy

D. Ireland, K. Livingston, J. Phillips[†], B. Seitz
University of Glasgow, Glasgow G12 8QQ, United Kingdom

H. Avakian[†], P. Rossi[1], C. Weiss
Jefferson Lab, Newport News, VA 23606, USA

A. Kotzinian
Istituto Nazionale di Fisica Nucleare, Sezione di Torino e Dipartimento di Fisica dell'Università, Torino, Italy

[*]Contact: mirazita@lnf.infn.it
[†]Co-spokesperson
[1]Secondary affiliation: *INFN - Laboratori Nazionali di Frascati*

G. De Cataldo, R. De Leo, D. Di Bari, L. Lagamba, E. Nappi, R. Perrino
Istituto Nazionale di Fisica Nucleare, Sezione di Bari e Dipartimento di Fisica dell'Università, Bari, Italy

S. Aiello, V. Bellini, M. De Napoli, A. Giusa, F. Mammoliti, E. Leonora, N. Randazzo, G. Russo, M. Sperduto, C. Sutera, C. Ventura
Istituto Nazionale di Fisica Nucleare, Sezione di Catania, Catania, Italy

L. Barion, G. Ciullo, M. Contalbrigo, P. Lenisa, A. Movsisyan, F. Spizzo, M. Turisini
Istituto Nazionale di Fisica Nucleare, Sezione di Ferrara e Dipartimento di Fisica dell'Università, Ferrara, Italy

F. De Persio, E. Cisbani, C. Fanelli, F. Garibaldi, F. Meddi, G. M. Urciuoli
Istituto Nazionale di Fisica Nucleare, Sezione di Roma e Gruppo Collegato Sanità, e Università La Sapienza, Italy

F. De Persio, E. Cisbani, C. Fanelli, F. Garibaldi, F. Meddi, G. M. Urciuoli
Istituto Nazionale di Fisica Nucleare, Sezione di Roma e Gruppo Collegato Sanità, e Università La Sapienza, Italy

A. D'Angelo, L. Colaneri L. Lanza, A. Rizzo, C. Schaerf, I. Zonta
Istituto Nazionale di Fisica Nucleare, Sezione di Roma-TorVergata e Dipartimento di Fisica dell'Università, Roma, Italy

G. Simi
Istituto Nazionale di Fisica Nucleare, Sezione di Padova, Padova, Italy

M. Carpinelli, V. Sipala
Università e Istituto Nazionale di Fisica Nucleare, 07100 Sassari, Italy

D. Calvo, A. Filippi
Istituto Nazionale di Fisica Nucleare, Sezione di Torino, Torino, Italy

Abstract

Hadron production in Semi-Inclusive Deep Inelastic Scattering (SIDIS) is generally studied in the Current Fragmentation Region, where the detected hadron originates from the struck quark. Conversely, in the Target Fragmentation Region (TFR), the hadron is produced in the fragmentation process of the target remnants. Here, the SIDIS process can be described trough the so-called Fracture Functions, which represent the joint probability of producing the final hadron from the target remnants when a parton of the target nucleon is struck by the virtual photon in a hard scattering process. Like the ordinary parton distribution functions, the Fracture Functions are universal objects, thus they can be measured in one experiment at a given hard scale and then used to make predictions for other experiments, at another hard scale.

We propose a study of these functions in the SIDIS electroproduction of Λ on a proton target, $ep \to e'\Lambda X$. This process has two main advantages: (i) the TFR can be cleanly identified and (ii) the weak decay $\Lambda \to p\pi^-$ provides a way of measuring the final hadron polarization, allowing access to all the relevant Fracture Functions. The TFR will be identified through the cut on the Feynman-x variable $x_F < 0$. The main focus of the proposal will be the measurement of the longitudinal spin transfer from the polarized beam to the Λ, which is sensitive to the ΔM^L Fracture Function, representing the probability of having a longitudinally polarized quark when a longitudinally polarized hadron is produced. Since the Λ spin mainly due to its strange quark, measurement of the Λ polarization can also provide information on the strange sea quark polarization in the nucleon. Measurements of the Lambda multiplicity will provide information on the unpolarized Fracture Function M. The study of its Q^2 dependence also will test the perturbative framework implied by Fracture Functions, simultaneously encoding the information on the interacting parton and on the fragmentation of the spectator system.

The measurements will be performed in the Hall B. We will use the 11 GeV polarized electron beam on an unpolarized hydrogen target and the CLAS12 detector to detect the scattered electron together with the proton and the pion from the Λ decay, with large coverage in the relevant kinematic variables. The CLAS12 central detector in particular will extend the detection of the low energy decay pion at large angles. The measurement will run simultaneously with the other approved experiments with unpolarized hydrogen target, thus no additional beam time is required.

Contents

1 Introduction **3**

2 Λ production in the target fragmentation region and Fracture Functions **4**

3 The polarization of the Λ in semi-inclusive production **6**

4 The cross section of the SIDIS production of polarized Λ **8**

5 Studies with CLAS at 5.5 GeV **11**

6 Studies with CLAS12 **15**

7 Projected Results **18**

8 Summary **20**

1 Introduction

The spin structure of the nucleon has been of central interest since the EMC [1] measurements implied that the helicity of the constituent quarks accounts for only a fraction of the nucleon spin. This so-called "spin crisis" was subsequently confirmed by a number of other experiments at CERN [2], SLAC [3, 4], HERA [5, 6] and JLab [7]. Possible interpretations of this result include a significant polarization of either the strange sea (negatively polarized) or the gluons (positively polarized). The contributions to the sum rule for the total helicity of the nucleon include the following:

$$\frac{1}{2} = \frac{1}{2}\sum_q \Delta q^{val} + \Delta q^{sea} + L_z^{val} + L_z^{sea} + L_z^{glue} + \Delta G,$$

where Δq, L_z and ΔG are respectively the quark helicity, the orbital angular momentum of all partons, and the gluon helicity.

One of the most remarkable results from semi-inclusive deep inelastic scattering (SIDIS) studies is the measurement by the HERMES collaboration of Δs being consistent with zero [5, 6], in contrast to expectations of $\Delta s \approx -0.1$ from DIS measurements. The origin of this negative sea polarization is likely nonperturbative and still has to be understood.

The analysis of QCD sum rules indicates that the condensate of $\bar{s}s$ pairs in the vacuum is not small, but is comparable with the condensate of the light quarks [8]. The strong attraction in the spin-singlet pseudoscalar channel may induce correlations between valence quarks from the proton wave function and vacuum antiquarks with opposite spins. Polarization measurements provide sensitive tests of models of strong–interaction dynamics. Measurements of the Λ polarization in SIDIS provide an important probe of the strange sea in the nucleon [9, 11] and may shed light on the proton spin puzzle. The advantage of detecting the Λ in the final state lies in the fact that its weak decay into $p\pi^-$ is self-analyzing. It can be used as a s quark polarimeter since the polarization of the Λ is defined by the polarization of its s quark.

Most of the Λ particles in the CLAS12 kinematics are in the Target Fragmentation Region (TFR) of DIS, which also carries interesting information about the spin and flavor structure of the nucleon but is still poorly understood and has not been studied systematically in experiments.

The main physical question in the TFR is how the diquark-like remnant system after the DIS process dresses itself up to become a full-fledged hadron, i.e., by which mechanism are the quark-antiquark pairs restoring color neutrality produced, and how this process is correlated with the spin of the target or/and the produced particles. In electroproduction, the polarized lepton emits a virtual photon with non–zero longitudinal polarization, which in turn selects preferentially one polarization state of the struck quark. The opposite polarization of a remnant $\bar{s}s$ pair can again be transferred to the final–state Λ polarization, with the efficiency extracted from eN collisions. After removing a polarized scattered quark from an unpolarized nucleon, the remnant diquark may combine with an s quark, which could originate from the nucleon sea or from a color string between the diquark and the scattered quark to form a Λ hyperon (see Fig. 1).

Significant polarization effects ($\sim 15-20\%$) have been predicted in Intrinsic Strangeness Model (ISM) for Λ production in the TFR in deep-inelastic scattering [10]. The sign of the

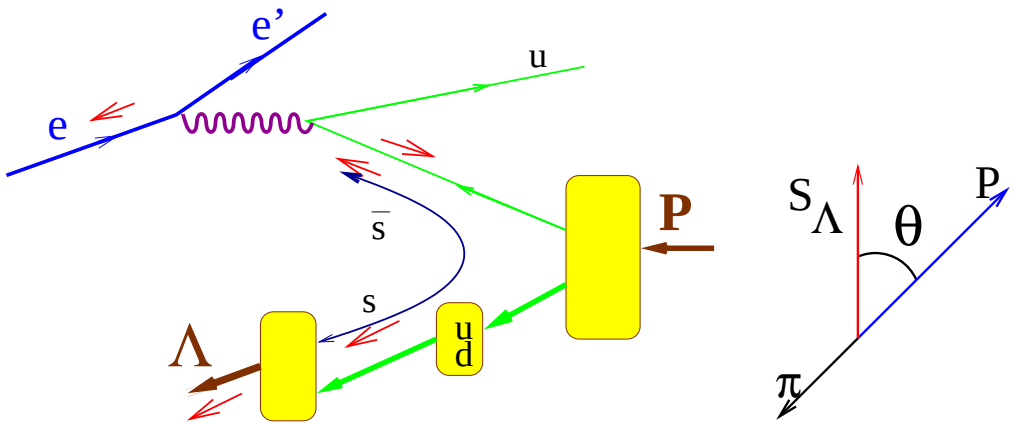

Figure 1: *Dominant diagram for* Λ *production in the target fragmentation region due to scattering on a valence u quark (left) and the* Λ *decay kinematics (right).*

polarization of Λ hyperons produced in the DIS of polarized charged-lepton off unpolarized nucleon depends on the sign of the beam polarization and was predicted to be positive for the positive lepton helicity.

The polarization of Λ hyperons in the target fragmentation region of DIS has also been considered in the meson cloud model [11]. Due to the pseudoscalar nature of the $NK\Lambda$ coupling, the polarization of final-state Λ hyperons was predicted to be strongly anticorrelated to that of the nucleon, thus vanishing for an unpolarized target.

Few experiments in SIDIS kinematics have measured the polarization transfer to Λ and $\bar{\Lambda}$, see Fig. 2, left and right plot respectively. The NOMAD experiment [12] used neutrino beams, while SLAC [13], Hermes [14] and COMPASS [15] used charged lepton beams. For the Λ, NOMAD is the only experiment that explored both the TFR and CFR. They found an enhancement of the polarization in the TFR ($P_\Lambda = 0.21 \pm 0.04(stat) \pm 0.02(syst)$ for $x_F < 0$) with respect to the CFR ($P_\Lambda = 0.09 \pm 0.06(stat) \pm 0.03(syst)$ for $x_F > 0$).

2 Λ production in the target fragmentation region and Fracture Functions

There is very little experimental data in the SIDIS target fragmentation region and a quantitative description of process occurring in this region of phase space relies on fragmentation models [16], although it is a potentially rich source of information on the properties of hadronization of the spectator system emerging from the hard collision. Its fragmentation is expected to be rather different from the hadronization mechaninsm of partons in the QCD vacuum, as for example in the DIS current fragmentation region, or e^+e^- annihilation.

It has been known for a long time [17] that the longitudinal momentum spectrum of particles produced in target fragmentation region exhibits some peculiar features that can be qualitatively accommodated within simple phenomenological rules. Only initial state particle whose valence-like parton content is almost conserved in the scattering can be the "leading" particle in the final state, *i.e.* carrying a substantial fraction of the incoming

hadron momentum. In fact, in ep interactions no leading particle effect is observed in the semi-inclusive production of mesons [20, 19] (see as an example Fig. 3) and recently confirmed also by CLAS results for π^+ [18], see Fig. 4. The differential cross-sections $d\sigma/dx_F$ rapidly fall off at large and negative x_F.

However, for baryon production, and in particular for Λ, a clear excess of yield with respect to mesons has been measured [19] for $x_F < 0$, as shown in the left plot of Fig. 3 A typical distribution in the target fragmentation region is of the type

$$d\sigma/dx_F \propto (1 - |x_F|)^n \tag{1}$$

with $n > 0$. Such behaviour has been also observed in the old semi-inclusive Λ production data measured at HERA [20] in a much lower beam energy range, comparable with the one of JLab.

In the context of pQCD, a quantitative study of Λ production in the target fragmentation region can be performed by using the formalism of Fracture Functions $M(x_B, \zeta)$ [21]. These distributions represent the probability of finding a parton of flavour i with fractional momentum x_B and a hadron h with fractional momentum ζ of the target nucleon N, respectively. Factorization theorems [22, 23] guarantee that Fracture Functions are universal distributions, at least in the context of SIDIS, and this fact constitutes a solid basis for phenomenological analysis. With respect to ordinary parton distribution functions, whose evolution is driven by the well known Altarelli-Parisi equations, these distributions obey a modified evolution equations [21], which take into account the different structure of collinear singularities in the target fragmentation region. Fracture functions do combine non-perturbative aspects of spectator fragmentation with well known behaviour of the evolution of the active parton which undergoes the hard collisions. Within this framework, higher orders for semi-inclusive unpolarized and polarized DIS have been calculated in Refs. [24, 25, 26] and asymmetries involving fracture functions has been studied in Ref. [27].

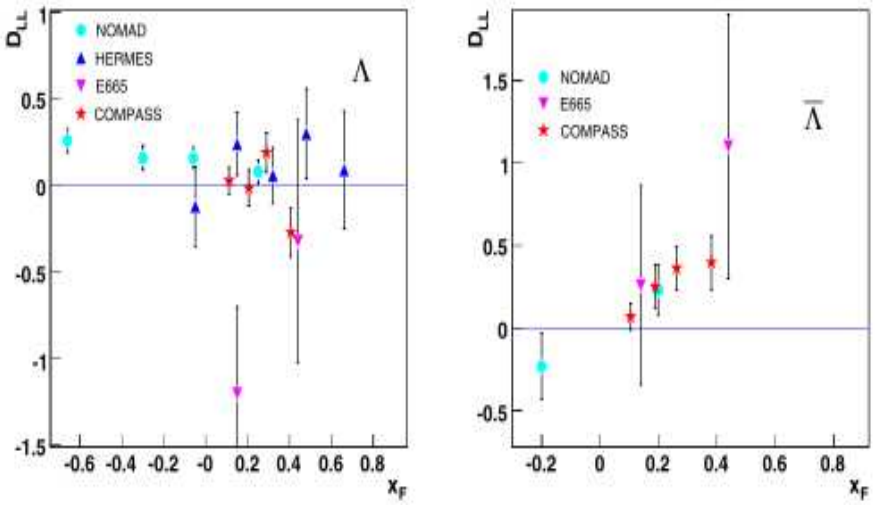

Figure 2: **Experimental measurements of the longitudinal Λ polarization transfer in SIDIS kinematics from NOMAD [12], SLAC [13], Hermes [14] and COMPASS [15] experiments.**

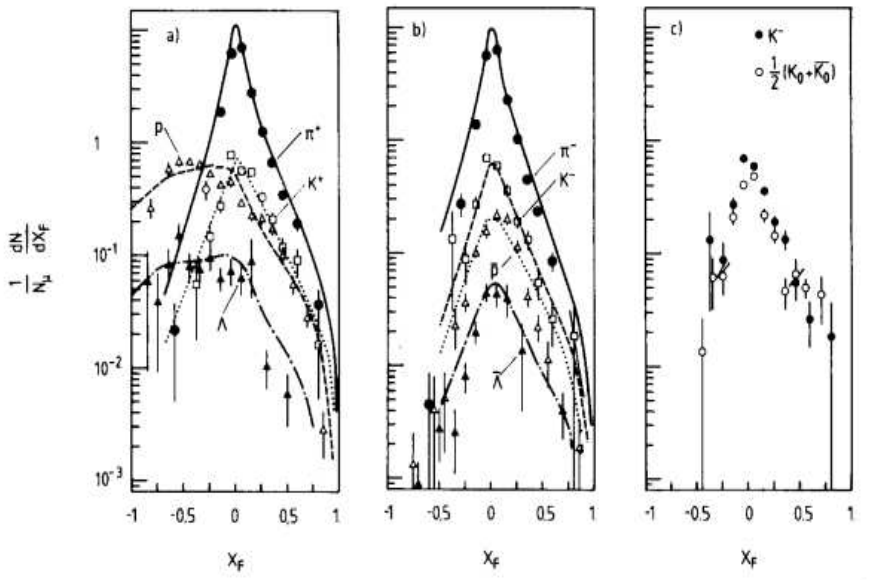

Figure 3: *Feynman x distributions normalized to the number of scattered muons measured by EMC [19] for positive and negative hadrons. (a) π^+, K^+, p and Λ, (b) π^-, K^-, $\bar{p}$ and $\bar{\Lambda}$, (c) K^- and $(K^0+\bar{K}^0)/2$. The curves represent the predictions of the Lund model.*

The fracture functions were originally introduced in the collinear limit and, in analogy with the Transverse Momentum Dependent (TMD) Parton Distribution Functions, they have been extended to include transverse momenta [28], although for these extended functions the factorization theorem has not yet been proved. The classification of all the leading-twist extended Fracture Function has been provided [29, 30].

3 The polarization of the Λ in semi-inclusive production

The kinematics of the SIDIS process

$$e(l)p(p_N) \to e'(l')\Lambda(p)X(p_X) \tag{2}$$

is represented in the Fig. 5 in the $\gamma^* p$ center of mass reference frame. The incoming and scattered electrons define the electron scattering plane, while the virtual photon and the Λ define the reaction plane. The azimuthal angle ϕ is the angle between these two planes, calculated according to the Trento convention [34].

The polarization of the Λ is defined in its rest frame. The coordinate system in this frame is the ($\hat{x}$, $\hat{y}$, $\hat{z}$) system of Fig. 5, with the longitudinal axis $\hat{z}$ parallel to the virtual photon direction, $\hat{y}$ normal to the electron plane and $\hat{x} = \hat{y} \times \hat{z}$.

In the SIDIS process, the polarization of the Λ (or of any spin-1/2 baryon) can be predicted on the basis of very general considerations. In fact [35], the hadron polarization

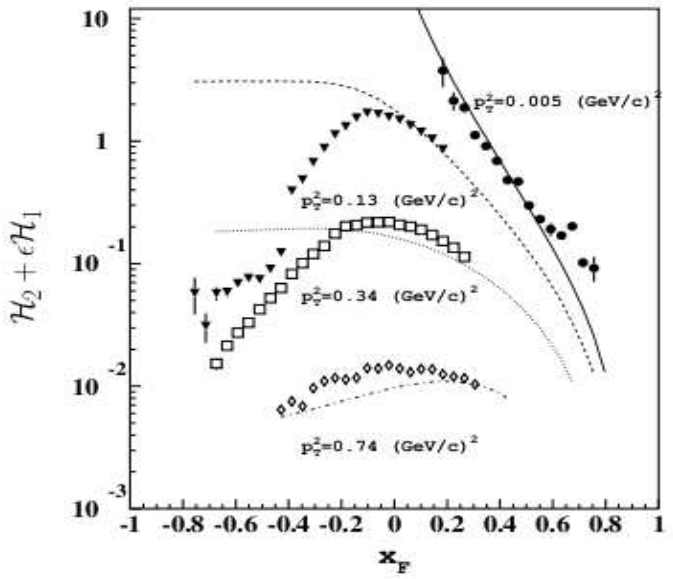

Figure 4: *The x_F -dependence of the structure function $H_1 + \epsilon H_@$ measured by CLAS for π^+ [18] at Q^2 = 2 (GeV/c)^2 and x_B = 0.26 at different values of the transverse momentum p_T.*

dependent part of the SIDIS cross section can be written as

$$\left(\frac{d\sigma}{d\Omega_{e'} d\Omega_\Lambda dE_{e'} dM_X}\right)_{pol} \propto S_\mu P_\Lambda^\mu \tag{3}$$

where $S_\mu = (1, S_x, S_y, S_z)$ is the spin projector operator in the $(\hat{x},\ \hat{y},\ \hat{z})$ frame and P_Λ^μ represent the Λ polarization. The cross section has to be a Lorentz scalar, invariant under parity transformation and linear in the spin. Thus, the possible scalar quantities that can

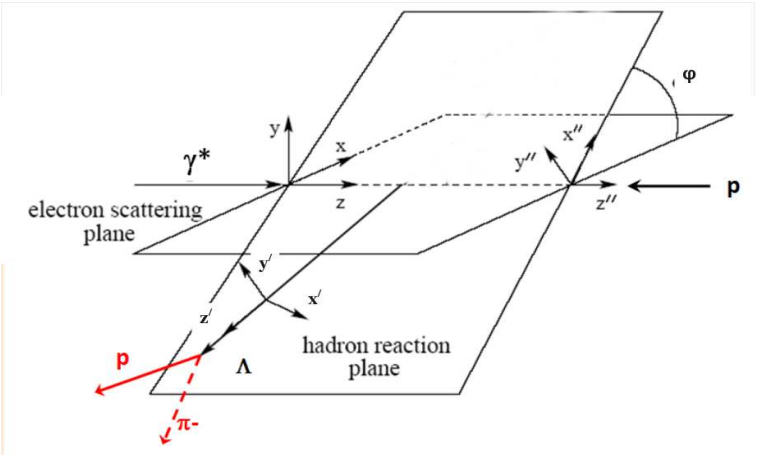

Figure 5: **Kinematic plane of the $ep \to e'\Lambda X$ reaction in the $\gamma^*\Lambda$ center of mass reference frame.**

be built from the available 4-vectors are (neglecting the target polarization):

$$\sigma_1 \propto \epsilon_{\mu\nu\alpha\beta} S^\mu l^\nu p_N^\alpha p^\beta \tag{4}$$

$$\sigma_2 \propto \epsilon_{\mu\nu\alpha\beta} S^\mu l'^\nu p_N^\alpha p^\beta \tag{5}$$

$$\sigma_3 \propto \epsilon_{\mu\nu\alpha\beta} S^\mu l^\nu l'^\alpha p^\beta \tag{6}$$

$$\sigma_4 \propto \epsilon_{\mu\nu\alpha\beta} S^\mu l^\nu l'^\alpha p_N^\beta \tag{7}$$

where $\epsilon_{\mu\nu\alpha\beta}$ is the totally antisymmetric tensor with $\epsilon_{0,1,2,3} = +1$.

After some algebra and isolating the coefficients of S_μ, the three components $i = x, y, z$ of Λ polarization P_Λ can be split into two components: the "induced" polarization, which is independent of the beam polarization, and the "transferred" polarization, which is dependent of the beam polarization

$$P_{\Lambda,i} = P^I_{\Lambda,i} + h P^T_{\Lambda,i} \tag{8}$$

being h the helicity of the incoming electron.

The induced part is given by

$$P^I_{\Lambda,x} = C^s_x \sin\phi + C^{s2}_x \sin 2\phi \tag{9}$$

$$P^I_{\Lambda,y} = C^0_y + C^c_y \cos\phi + C^{c2}_x \cos 2\phi \tag{10}$$

$$P^I_{\Lambda,z} = C^s_z \sin\phi + C^{s2}_z \sin 2\phi \tag{11}$$

while the transferred part is given by

$$P^T_{\Lambda,x} = D^0_x + D^c_x \cos\phi \tag{12}$$

$$P^T_{\Lambda,y} = D^s_y \sin\phi \tag{13}$$

$$P^T_{\Lambda,z} = D^0_z + D^c_z \cos\phi \tag{14}$$

All the 7+5 coefficients C^m_i and D^m_i are (unknown) functions of all the relevant kinematics variables like Q^2, x_B or ζ.

4 The cross section of the SIDIS production of polarized Λ

From the kinematic point of view, referring to the momenta defined in eq. (2), the SIDIS process is described by the invariants

$$x_B = \frac{Q^2}{2 p_N \cdot q} \tag{15}$$

$$y = \frac{p_N \cdot q}{p_N \cdot l} \tag{16}$$

$$z_\Lambda = \frac{p_N \cdot p}{p_N \cdot q} \tag{17}$$

$$W^2 = (p_N + q)^2 \tag{18}$$

being $q = l - l'$ the virtual photon 4-momentum and $Q^2 = -q^2$. In the Fracture Function formalism, the variable z_Λ is usually replaced by the variable $\zeta = z_\Lambda(1-x_B)$. The production of a hadron h in the final state can originate from the struck parton or from the target remnants, so that

$$\sigma = \sigma^{CFR} + \sigma^{TFR} \tag{19}$$

These two contributions are schematically represented in Fig. 6.

The separation between CFR and TFR is done by means of the Feynman variable $x_F = 2p_\parallel^{CM}/W$ (here $p_\parallel^{CM}$ is the projection of the Λ momentum on the virtual photon momentum in the $\gamma^* p$ center of mass frame): hadrons with $x_F > 0$ are produced in the CFR while hadrons with $x_F < 0$ are produced in the TFR. Additional cuts on z_Λ or ζ may be used to further suppress the target fragmentation contribution for $x_F > 0$.

In the CFR, the SIDIS cross section can be written in terms of Transverse Momentum Dependent (TMD) parton and fragmentation functions, and, after integration of all the transverse momenta, following ref. [29], we have

$$\begin{aligned}
\frac{d\sigma^{CFR}}{dx_B dy dz_\Lambda d\phi_S d\phi} &= \frac{\alpha_{em}^2}{\pi Q^2 y} \sum_a e_a^2 \\
&\left\{ \left(1 - y + \frac{y^2}{2}\right) \left[f_1(x_B) G_1(z_\Lambda) + S_{N\parallel} S_\parallel g_1(x_B) G_1(z_\Lambda) \right] \right. \\
&- (1-y) \left| \mathbf{S}_{N\perp} \right| \left| \mathbf{S}_\perp \right| h_1(x_B) H_1(z_\Lambda) \cos(\phi + \phi_S) \\
&\left. + hy \left(1 - \frac{y}{2}\right) \left[S_{N\parallel} g_1(x_B) D_1(z_\Lambda) + S_\parallel f_1(x_B) G_1(z_\Lambda) \right] \right\}
\end{aligned} \tag{20}$$

where $\mathbf{S}_N$ is the target nucleon spin and ϕ_S the azimuthal angle of its transverse component, $\mathbf{S}$ is the Λ spin, f_1, g_1 and h_1 are the leading twist parton distribution functions, D_1, G_1 and H_1 are the leading twist fragmentation functions and the sum runs over the quark flavours a

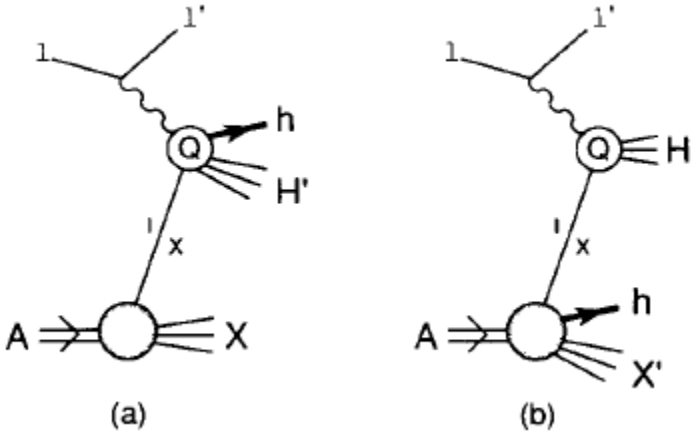

Figure 6: **Semi inclusive production of the hadron h in the current (a) and target (b) fragmentation regions.**

with electric charge e_a (note that in the distribution and fragmentation function the flavour index has been omitted).

In the TFR, the Fracture Function expression of the cross section, after transverse momenta integration, can be written as [29]

$$\begin{aligned}
&\frac{d\sigma^{TFR}}{dx_B dy d\zeta d\phi_S d\phi} = \\
&= \frac{\alpha_{em}^2}{\pi Q^2 y} \sum_a e_a^2 \times \\
&\left\{ \left(1 - y + \frac{y^2}{2}\right) \left[M(x_B,\zeta) + S_{N\parallel} S_\parallel M_L^L(x_B,\zeta) + |\mathbf{S}_{N\perp}|\,|\mathbf{S}_\perp|\, M_T^T(x_B,\zeta)\cos\left(\phi - \phi_S\right) \right] \right. \\
&+ hy \left(1 - \frac{y}{2}\right) \left[S_{N\parallel} \Delta M_L(x_B,\zeta) + S_\parallel \Delta M^L(x_B,\zeta) + \right. \\
&\left. \left. + |\mathbf{S}_{N\perp}|\,|\mathbf{S}_\perp|\, \Delta M_T^T(x_B,\zeta)\sin\left(\phi - \phi_S\right) \right] \right\}
\end{aligned} \tag{21}$$

Here, the six fracture functions (for each quark flavour a) depend on the Bjorken variable x_B and on the variable ζ which represents the fraction of the nucleon longitudinal momentum carried by the final hadron. There are three sets of fracture functions, namely M, ΔM and $\Delta_T M$ for unpolarized, longitudinally or transversely polarized quarks, the latter not contributing to the SIDIS process. Each fracture function can have a subscript L or T for longitudinally or transversely polarized nucleon target, and similarly for the superscript referring to the final hadron polarization. While in the CFR there is only one azimuthal modulation of the type $\cos(\phi + \phi_S)$, in the TFR two modulations are present: the first is a $\cos(\phi - \phi_S)$ and involves unpolarized quarks and the second is $\sin(\phi - \phi_S)$ and involves longitudinally polarized quarks. The measurement of non-zero modulations of this type would be a clear evidence of a target fragmentation process.

Neglecting the target polarization (hence integrating over ϕ_S), the 4-fold differential cross sections of eqs. (20,21) can be written as

$$\frac{d\sigma}{d\vec{X}} = \sigma_0 \left(1 + h S_\parallel A_{LUL}\right) \tag{22}$$

where σ_0 is the unpolarized (CFR or TFR) cross section and the spin-dependent terms A_{LUL} (with the three subscripts refer to unpolarized (U) or longitudinally polarized (L) beam, target and final hadron) are given by

$$A_{LUL}^{CFR} = h S_\parallel \frac{y\left(1 - \frac{y}{2}\right) \sum_a e_a^2 f_1 G_1}{\left(1 - y + \frac{y^2}{2}\right) \sum_a e_a^2 f_1 D_1} \tag{23}$$

and

$$A_{LUL}^{TFR} = h S_\parallel \frac{y\left(1 - \frac{y}{2}\right) \sum_a e_a^2 \Delta M^L}{\left(1 - y + \frac{y^2}{2}\right) \sum_a e_a^2 M} \tag{24}$$

The kinematic factor $D(y) = y(1 - y/2)/(1 - y - y^2)$ is the depolarization factor and accounts for the polarization transfer from the initial electron to the virtual photon. No

ϕ modulation are contributing, because they arise from the correlation between the target and Λ spins. By comparing with the general expression of the Λ polarization in SIDIS, eqs. (9-14), we see that at leading twist the only non zero term is D_z^0, all the remaining terms vanishing after integration over transverse momenta or being higher twist.

Unfolding from eq. (24) the beam polarization and the depolarization factor, one can obtain the polarization transfer coefficient

$$D^{LL} = \frac{\sum_a e_a^2 \Delta M^L}{\sum_a e_a^2 M} \tag{25}$$

Detection of the forward going Kaon, produced in the current fragmentation region combined with detected Lambda in the target fragmentation region in case of a longitudinally polarized lepton beam may provide access to fracture functions of longitudinally polarized quarks inside the unpolarized nucleon [30, 31]. The observation and measurement of the predicted azimuthal dependences in the TFR would allow the extraction of the fracture functions, similarly to what is being done for TMDs in the CFR.

5 Studies with CLAS at 5.5 GeV

The Λ longitudinal polarization transfer in SIDIS process has been measured using the *e1f* data set taken with the CLAS detector. The electron beam had energy of 5.5 GeV and average polarization $P_B = 0.74 \pm 0.03$ and was scattered off an unpolarized, 5 cm long, liquid hydrogen target.

The Λ particle was detected through its charged decay $\Lambda \to p\pi^-$, and the two hadrons, together with the scattered electrons, were detected in CLAS. The DIS region was selected through the cuts $Q^2 > 1$ GeV^2 and $W^2 > 5$ GeV^2. The invariant mass distribution of the proton and pion is shown in Fig. 7 and the signal region is defined by the cuts $M \pm 3\sigma$.

The missing mass of $e\Lambda X$ events is shown in Fig. 8. A prominent peak of exclusive $e\Lambda(K^+)$ can be seen, accounting for about 30% of the total produced Λ. After this exclusive peak, there is a broad distribution of events, with a smaller peak at $MM \approx 0.9$ GeV corresponding to the exclusive $e\Lambda(K^*(890)^+)$ events. The latter events contribute to about 10% of the total statistics.

Because of the large contribution of the $e\Lambda(K^+)$, which are most likely to have been produced through different mechanisms than that described by the Fracture Functions (for example GPDs), the final sample of inclusive Λ events were selected by a cut $MM > 0.65$ GeV. Nevertheless, the missing mass dependence of the measured polarization has been studied.

Monte Carlo simulations of the process have been performed using the **clasDIS** [38] generator, which is based on the PYTHIA and JETSET [39] simulation codes. Some of the parameters of the JETSET part of the code (governing the fragmentation of the quarks into the final hadrons) have been tuned by comparing with the experimental distributions. The CLAS response has been simulated through the GSIM simulation code, calibrated for the *e1f* data set. Good agreement between data and Monte Carlo has been obtained for several kinematic distributions, as shown in fig. 9.

The Λ polarization can be directly measured through the angular distribution of its weak decay $\Lambda \to p\pi^-$. In fact, the proton angular distribution can be written as

$$\frac{dN}{d\cos\theta_p^*} \propto 1 + \alpha P_\Lambda \cos\theta_p^* \tag{26}$$

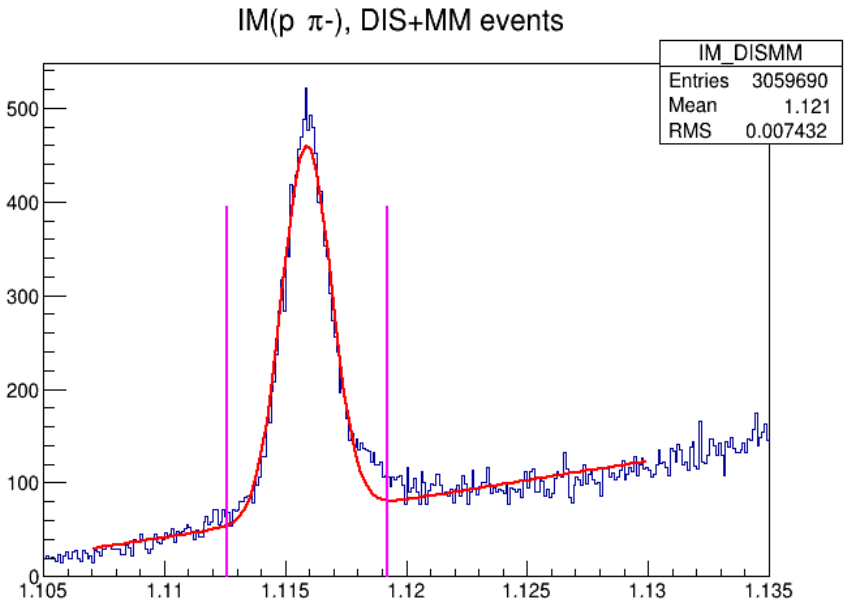

Figure 7: **Invariant mass of proton and π^- for $ep\pi^-X$ events.**

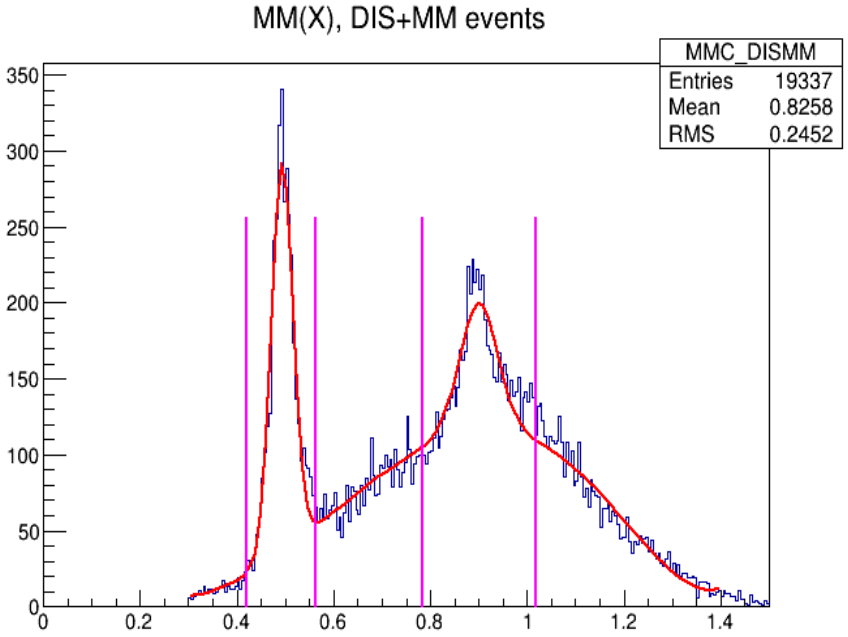

Figure 8: **Missing mass of $ep \to e\Lambda X$ events after DIS cuts.**

where θ_p^* is the proton emission angle in the Λ rest frame and P_Λ the Λ polarization, both projected onto the relevant axis in the frame described in Sect. 3.

The only non-zero leading-twist component of the polarization (see eq. (14)) is proportional to the beam helicity, thus it can be easily extracted measuring the Beam Spin Asymmetry. In a given $\cos\theta_p^*$, one can define the asymmetry

$$A = \frac{N^+ - N^-}{N^+ + N^-} \tag{27}$$

and then a linear fit in $\cos\theta_p^*$ provides the slope of the dependence in eq. (26).

The (preliminary) measured polarization transfer coefficient D^{LL} as a function of x_F is shown in Fig. 10. We see a quite large polarization, up to about 30% in the target

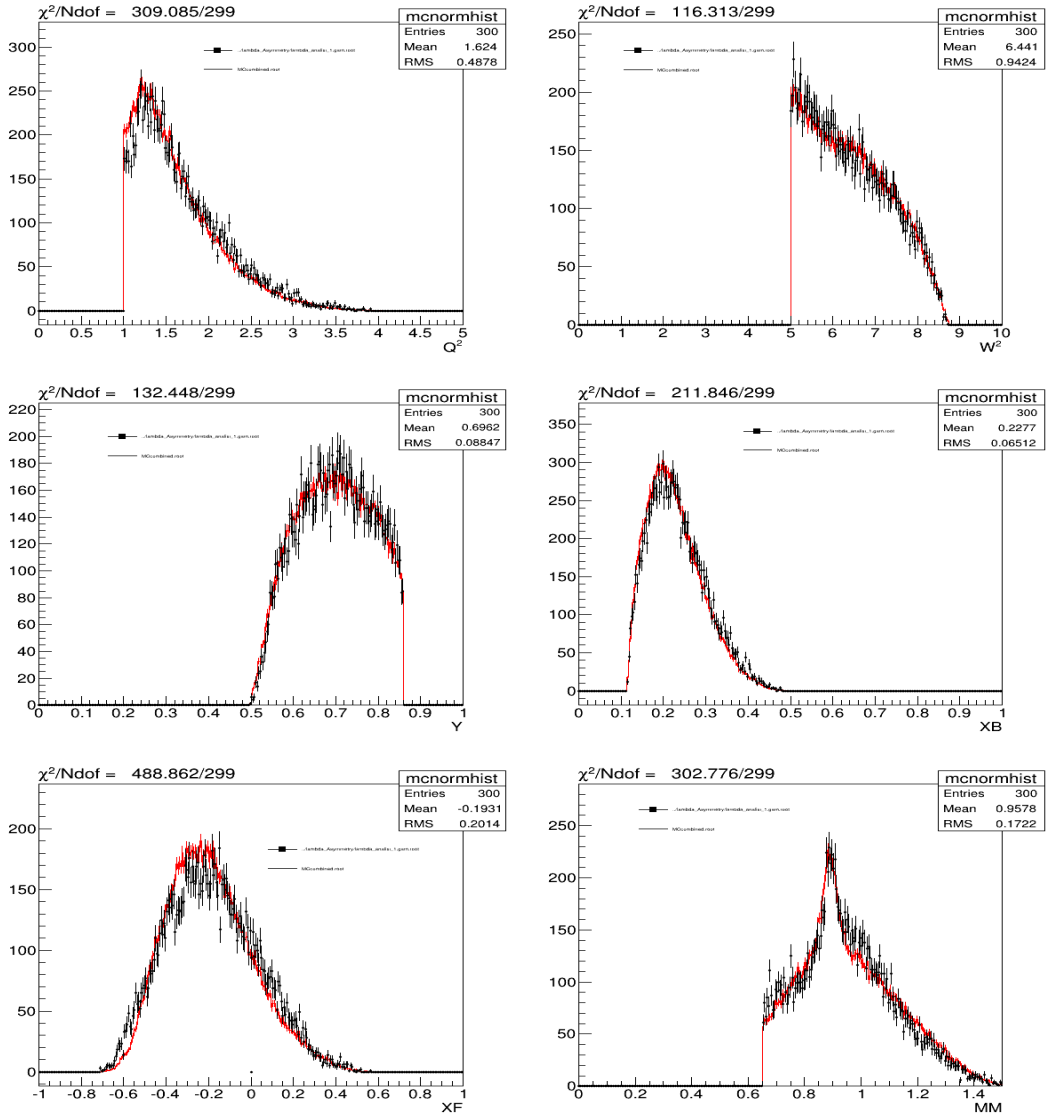

Figure 9: **Comparison between experimental (black points) and Monte Carlo (red histogram) distributions for several kinematics quantities for $e\Lambda X$ events after DIS and missing mass cuts measured with 5.5 GeV electron beam at CLAS.**

fragmentation region ($x_F < 0$), while the polarization is consistent with zero, even if with large error bars, in the current fragmentation region ($x_F > 0$). In the TFR, the results are systematically higher but, within the errors, consistent with the ISM predictions [10].

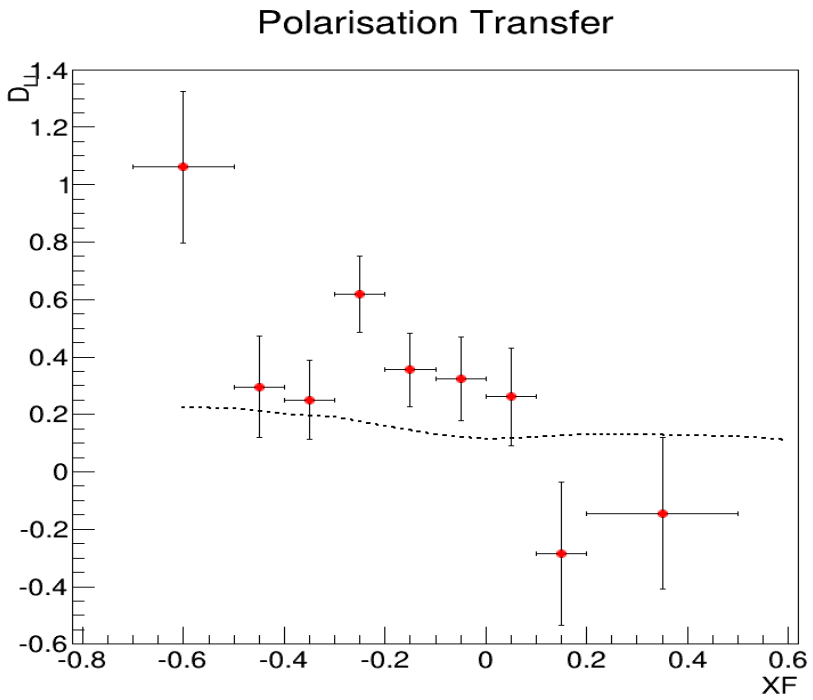

Figure 10: **Longitudinal Λ polarization transfer coefficient as a function of x_F measured with 5.5 GeV electron beam at CLAS (preliminary), compared with the ISM prediction [10] (dashed line).**

6 Studies with CLAS12

The same **clasDIS** Monte Carlo generator was also used to study the Λ SIDIS electroproduction with a 11 GeV beam. Since no experimental data are available at these energies, the JETSET parameter tuning made by the Hermes experiment has been adopted. The CLAS12 response has been simulated using the Fast-MC code, which gives a reasonable description of the expected detector performances. The generated events have been processed considering both torus field polarities.

The analysis procedure closely follows that of the 5.5 GeV CLAS data, described in the previous section. The DIS cuts $Q^2 > 1$ GeV^2 and $W^2 > 5$ GeV^2 are applied and the Λ is identified in the invariant mass distribution of its decay proton and pion, as shown in Fig. 11 for the two torus field polarities. We see for reversed field not only a better resolution (σ=0.5 MeV) compared to normal field (σ=0.8 MeV) but also a much bigger number of reconstructed Λs (we recall that the two plots are produced from the same generated event sample).

The reason of the difference is clear in the Fig. 12. With reversed field, CLAS12 has a much bigger acceptance for large missing mass events, because of the better coverage for the low energy pions produced in the Λ decay, as shown in the left plot of Fig. 13. On the other hand, a slightly better acceptance is found with normal field polarity at large negative values of x_F, see the right plot in Fig. 13. A scatter plot of x_F as a function of ζ is shown in Fig. 14, we see that for $x_F < 0$ the values of ζ never exceed 0.5.

From the physics interpretation point of view, the question may arise whether large contributions from exclusive channels or the Λ produced in the decay of heavier hyperons should be removed or not. The physics process leading to the Fracture Function definition (see Fig. 6) requires an inclusive measurement including all the partial reaction channels. On the other hand, it may happen that specific channels, produced through different reaction mechanisms, may contribute significantly to the final sample of detected Λ. This was the case of the exclusive $e\Lambda K^+$ final state in the 6 GeV CLAS analysis. Thus, looking at the partial channels may give interesting information on the dynamics of the process, and, thanks to its excellent PID capabilities, CLAS12 will allow these kind of studies.

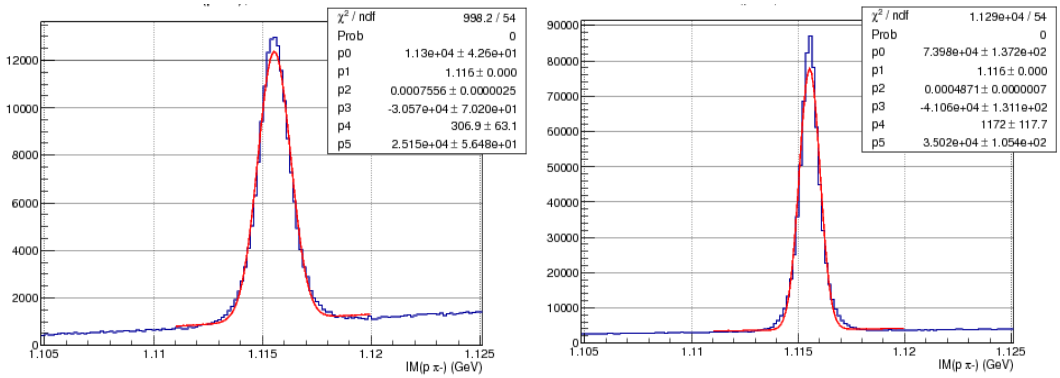

Figure 11: **Invariant mass of proton and π^- for $ep\pi^-X$ events from ClasDIS and Fast-MC simulations with 11 GeV electron beam for normal (right) and reversed (left) torus field polarity.**

Besides exclusive channels, the Λ can be produced in the decay of heavier hyperons, for example $\Sigma^0 \rightarrow \Lambda\gamma$ or $\Sigma^+(1385) \rightarrow \Lambda\pi^+$. The contribution of Λ coming from Σ^0 decay is shown in the Fig. 15 by looking at the $MM(e\Lambda X)$ distribution from generated events. Is is over the whole missing mass range of the order of 10%.

The Σ^0 may be anyway reconstructed by looking at the invariant mass of the Λ and of one photon detected in the CLAS12 calorimeters. The simulations (see Fig. 16 for the reversed torus field setting) show that a significant fraction of the decay photons have energy high

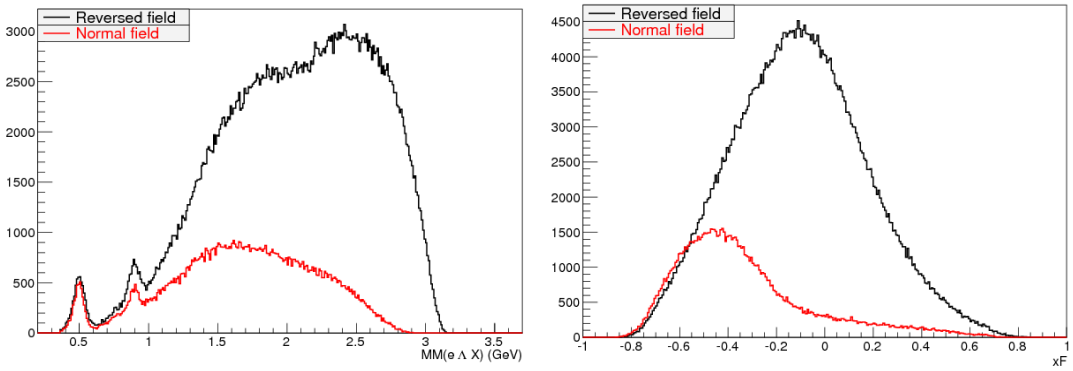

Figure 12: **Missing mass (left) and x_F distributions of $e\Lambda X$ events from ClasDIS and Fast-MC simulations with 11 GeV electron beam for the two torus field polarities.**

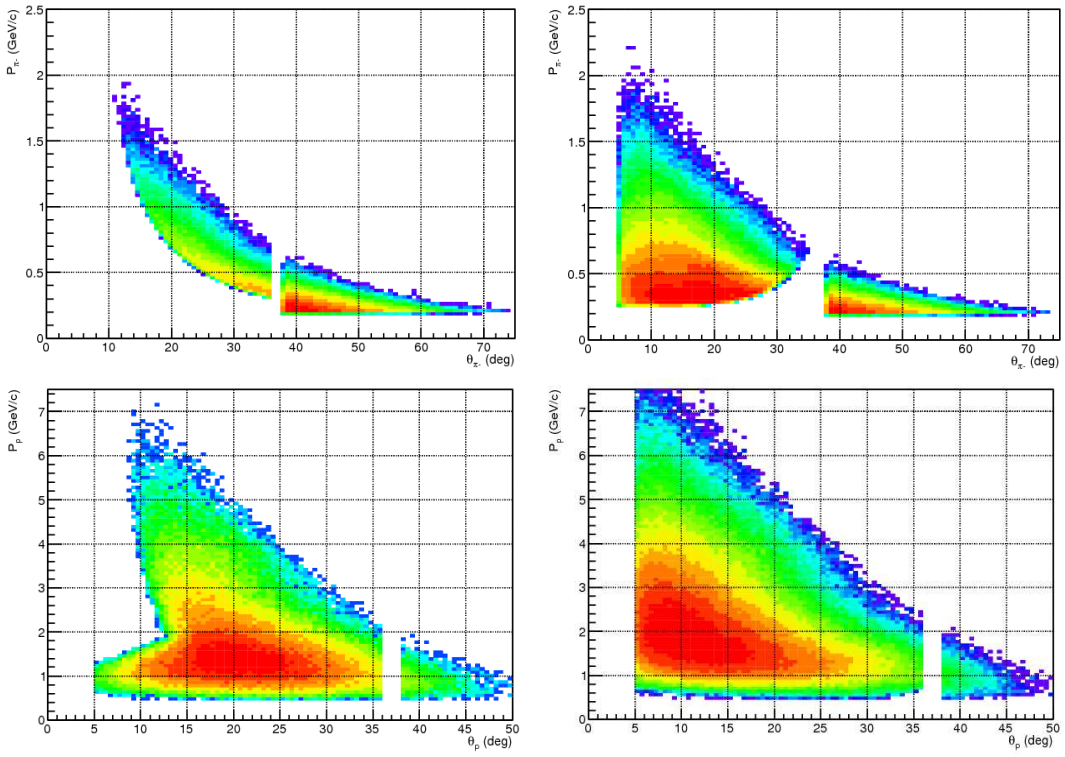

Figure 13: **Kinematic coverage of π^- (upper plots) and protons (lower plots) in $e\Lambda X$ events from ClasDIS and Fast-MC simulations with 11 GeV electron beam for normal (right) and reversed (left) torus field polarity.**

enough to be detected. The background in the invariant mass distribution of the right plot of Fig. 16 can be largely reduced by properly selecting the final sample of events, thus allowing the measurement of the polarization of the Σ^0, though with smaller statistical precision.

Similarly, in Fig. 17 we show the invariant mass distribution of $\Lambda\pi^+$ pairs, where the

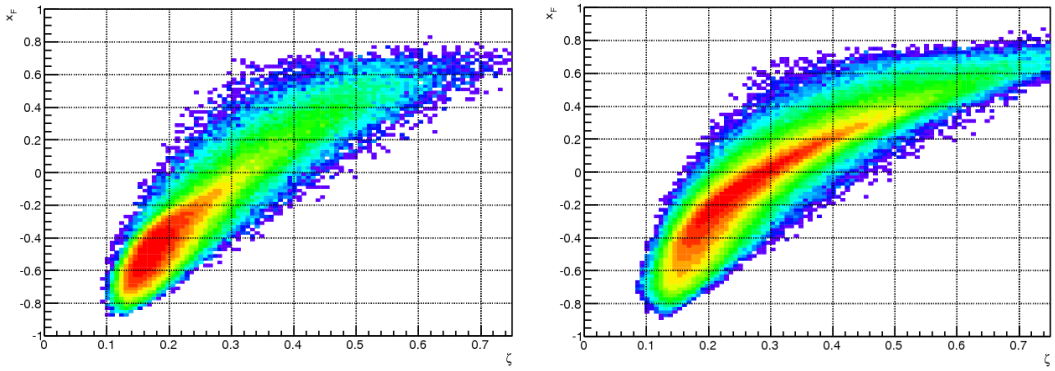

Figure 14: **Scatter plot of x_F versus ζ in $e\Lambda X$ events from ClasDIS and Fast-MC simulations with 11 GeV electron beam for normal (right) and reversed (left) torus field polarity.**

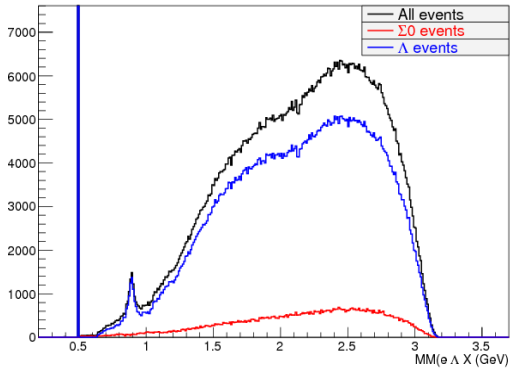

Figure 15: **Missing Mass distribution from generated events (black histogram) and contributions from primary Λ (red histogram) and from Σ^0 decays (blue histogram)**

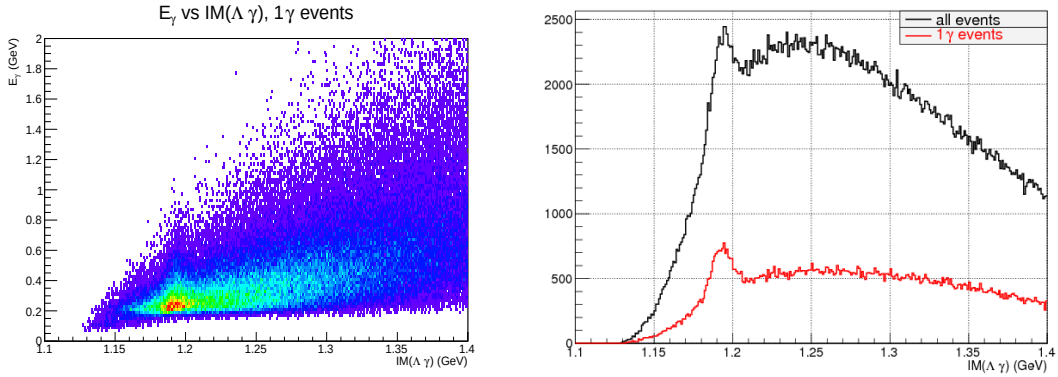

Figure 16: **Photon energy versus the reconstructed Σ^0 invariant mass from the $\Sigma^0 \to \Lambda\gamma$ decay (left plot) invariant mass projection (right plot: black histogram for all events; red histogram for events with only one detected photon). Simulation with reversed torus field polarity.**

peak of the $\Sigma^+(1385)$ is clearly visible. The fraction of Λ produced through the $\Sigma^+(1385)$ decay represents few percent of the total.

7 Projected Results

The proposed measurements requires an electron beam of 11 GeV with high polarization and an unpolarized hydrogen target. Other already approved experiments (for example E12-09-008 or E12-06-112) will have the same running conditions, with half of data taking with normal polarity and half with reversed polarity of the torus field, thus no new running time is necessary for our measurements. In addition, no special trigger requirements are necessary. The SIDIS measurements usually use a *one-electron* trigger (i.e. a hit in the High Threshold Cherenkov Counter in coincidence with the Electromagnetic Calorimeter in the same sector). A more strict trigger condition as for example one electron plus one charged particle is equally fine, because two opposite charge hadrons are always necessary to reconstruct the Λ.

For the calculation of the projected errors, we assume 60 days of data taking (E12-06-112). Because of the much bigger acceptance with reversed torus field, the estimate of the foreseen statistical errors are computed only for this setting and considering half of the approved running time. A further scaling of the running time by a factor of 3 has been applied, to take into account other contributions that may reduce the figure-of-merit of the measurement (as for example the trigger efficiency, the beam polarization, and so on).

The Fracture Functions depend upon the two variables x_B and ζ. The unpolarized Fracture Function $M(x_B, \zeta)$ can be accessed through the measurement of the differential cross section or of the Λ multiplicity, i.e. the unpolarized cross section normalized to the number of DIS electrons. The statistical precision of these measurement in the x_B vs ζ plane is shown in Fig. 18. It is well below 10% in the whole kinematic plane. This small statistical error will allow to study the x_B and ζ dependence of the Λ production as a function of x_F, in order to analyze the transition from the CFR to the TFR.

The procedure to compute the expected statistical precision of the extraction of the Λ longitudinal polarization transfer coefficient is the same used with the 5.5 GeV CLAS data.

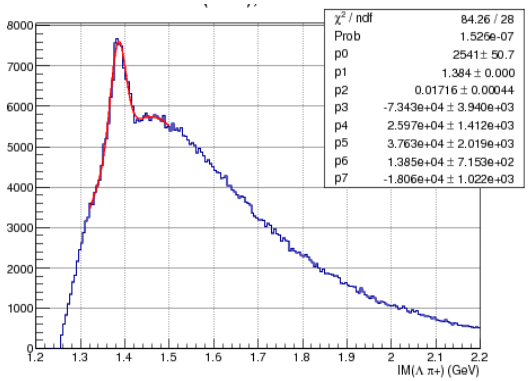

Figure 17: **Invariant mass distribution of the $\Lambda\pi^+$ pairs with fit of the $\Sigma^+(1385)$ peak. Simulation with reversed torus field.**

We assume a constant $D^{LL} = 0.3$ (roughly the value obtained in the TFR from the e1f data), we then generate accordingly the beam helicity in the Monte Carlo data and we compute the Beam Spin Asymmetry, eq. (27). An example of the reconstructed Λ mass distributions obtained for the two generated helicity states for the bin $x_F = -0.55$ and $\cos(\theta_p) = 0.5$ is shown in the left plot of Fig. 19. A fit of these distributions with a gaussian plus a polynomial is used to subtract the background and to obtain the number of Λ. Then the asymmetry is computed using eq. (27) and finally its $\cos(\theta_p)$ dependency is fitted with a straight line to extract from the fitted slope the Λ polarization using eq. (26). An example of the fit for the bin $x_F = -0.25$ is shown in the right plot of Fig. 19.

In Fig. 20, we show the projected results for the x_F dependence, compared with the e1f results and the ISM predictions [10]. An improvement by a factor bigger than 10 in the statistical precision with respect to the e1f results can be obtained. In Fig. 21, we show the missing mass and x_B dependencies in the TFR, with the cut $x_F < 0$.

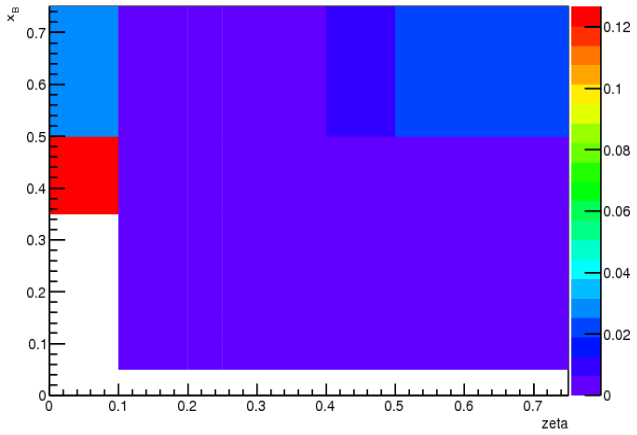

Figure 18: **Relative statistical error on the extraction of the unpolarized $M(x_B, \zeta)$.**

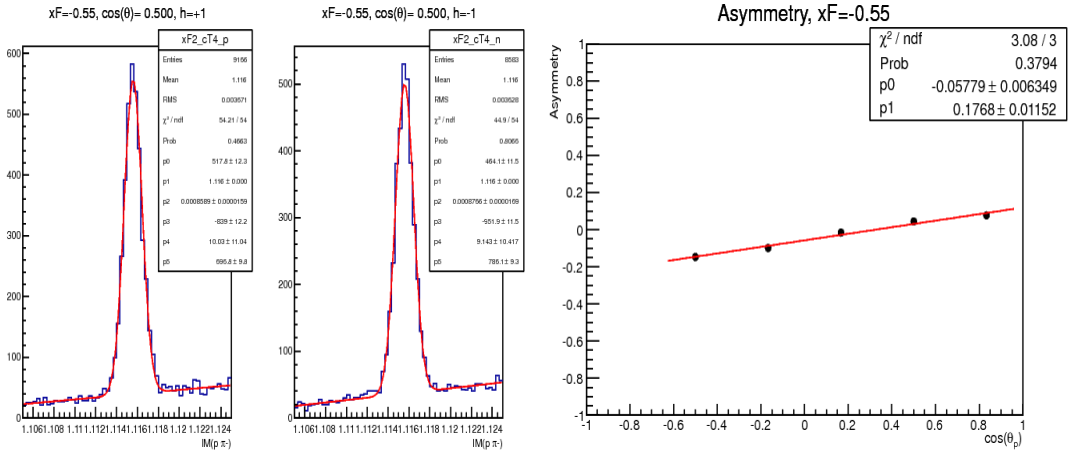

Figure 19: **Left plot: simulated Λ mass distribution for the two helicity states in the bin $x_F = -0.55$ and $\cos(\theta_p) = 0.5$. Right plot: asymmetry as a function of $\cos(\theta_p)$ for the bin $x_F = -0.55$.**

Multidimensional binning in the analysis will also be possible. As an example, we show in Fig. 22 the projected polarization results as a function of x_B at fixed ζ for $x_F < 0$.

The high statistical precision of the data will allow the use of more refined analysis tools. For example, by performing an unbinned likelihood fit of the event distributions one may in principle extract at the same time all the allowed modulations of the Λ polarization discussed in Sect. 3 and test the leading-twist expansion of eq. (21) with only the D_z^0 term being non-zero. The tuning of these new tools is currently under development with the 5.5 GeV CLAS data.

8 Summary

In this experiment we propose a study of the semi-inclusive electroproduction of the Λ. The run conditions, maximum electron beam energy and unpolarized hydrogen target, are the same as for the experiment E12-09-008 and E12-06-112, thus no additional running time is requested. In addition, no special trigger is required for this measurement.

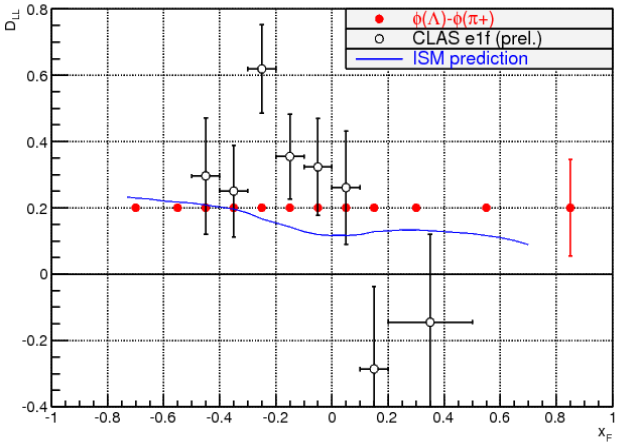

Figure 20: **Projected results of the longitudinal spin transfer as a function of x_F (red full circles) compared with the e1f data and the ISM prediction [10]**

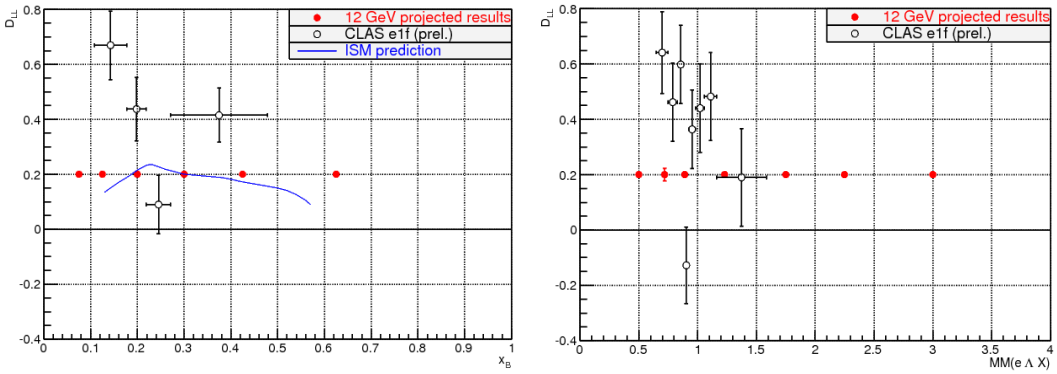

Figure 21: **Projected results of the longitudinal spin transfer as a function of x_B and of the missing mass (red full circles) compared with the e1f data and the ISM prediction [10]**

The high luminosity and the large acceptance of the CLAS12 detector will allow the acquisition of an amount of data more than an order of magnitude higher than all the experiments performed so far. This will allow multidimensional studies of the Λ polarization with high statistical accuracy in the target fragmentation region. These data will provide important inputs for the understanding of the Fracture Function, the underlying distribution functions describing the SIDIS physics in the TFR. The current fragmentation region will also be measured, even if with lower statistical accuracy due to the CLAS12 acceptance. The comparison between the two regions will be important to better understand their separation in terms of the available kinematic variables.

References

[1] J. Ashman *et al.*, [EMC Collaboration], Phys. Lett. **B206**, 364 (1988); Nucl. Phys. **B328** (1989) 1.

[2] D. Adams *et al.*, [SMC Collaboration], Phys. Rev. **D56**, 5330 (1997); B.Adeva *et al.*, [SMC Collaboration], Phys. Lett. **B420**, 180 (1998).

[3] K. Abe *et al.*, [E143 Collaboration], Phys. Rev. **D58**, 112003 (1998).

[4] P. L. Anthony *et al.*, [SLAC E155 Collaboration], Phys.Lett. **B458**, 529 (1999).

[5] K. Ackerstaff *et al.*, [HERMES Collaboration], Phys. Lett. **B464**, 123 (1999).

[6] HERMES collaboration (A. Airapetyan *et al.*), hep-ex/0407032.

[7] R. Fatemi *et al.*, [CLAS Collaboration], Phys. Rev. Lett. **91**, 22203 (2003).

[8] B.L. Ioffe, *Nucl. Phys.* **B188** (1981) 317

[9] J. Ellis, D. E. Kharzeev and A. Kotzinian, Z. Phys. **C69** 467 (1996).

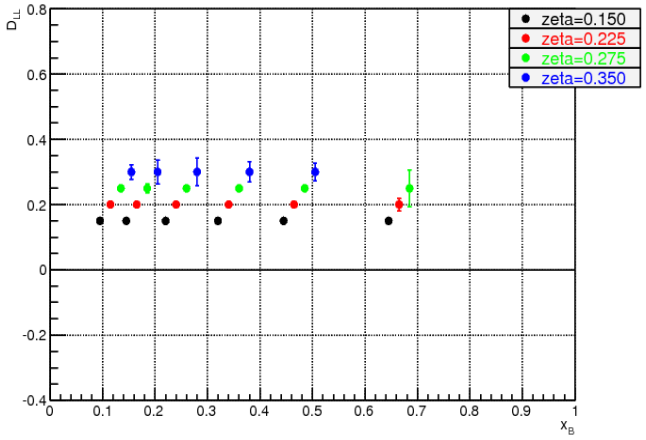

Figure 22: **Projected results of the longitudinal spin transfer at fixed ζ as a function of x_b (the points are slightly shifted for the clarity of the figure).**

[10] J. Ellis, A. Kotzinian, D. Naumov and M. Sapozhnikov, Eur. Phys. J. **C 52** 283 (2007).

[11] W. Melnitchouk and A. W. Thomas, Z. Phys. **A353** 311 (1996).

[12] P. Astier *et al.*, Nucl. Phys. **B588** 3 (2000); Nucl. Phys. **B605** 3 (2001).

[13] M.R. Adams *et al.*, Eur. Phys. J. **C 17** 263 (2000).

[14] A. Airapetien *et al.*, Phys. Rev. **D74** 072004 (2006).

[15] M. Alekseev *et al.*, Eur. Phys. J. **C 64** 171 (2009).

[16] B. Andersson, G. Gustafson, G. Ingelman, T. Sjostrand, Phys.Rept.97, 31 (1983).

[17] M. Basile & al, Nuovo Cim.A66 (1981) 129.

[18] M. Osipenko & al, (CLAS Collaboration) Phys.Rev.D80, 032004 (2009).

[19] EMC Collaboration, (M. Arneodo et al) Phys. Lett. B150, 458 (1985).

[20] I. Cohen & al, Phys.Rev.Lett.40, 1614 (1978).

[21] L. Trentadue and G. Veneziano, Phys. Lett. B323, 201 (1994).

[22] J. C. Collins, Phys.Rev.D57, 3051 (1998).

[23] M. Grazzini, L. Trentadue, G. Veneziano, Phys.B519, 394 (1998).

[24] D. Graudenz, Nucl. Phys. B432, 351 (1994).

[25] D. de Florian et al Nucl. Phys. B470, 195 (1996).

[26] D. de Florian, R. Sassot, Nucl. Phys. B488, 367 (1997).

[27] D. de Florian et al., Phys.Lett.B389, 358 (1996).

[28] F.A. Ceccopieri, L. Trentadue, Phys. Lett **B636**, 310 (2006).

[29] M. Anselmino, V. Barone and A. Kotzinian, Phys. Lett. B **699**, 108 (2011).

[30] M. Anselmino, V. Barone and A. Kotzinian, Phys. Lett. B **706**, 46 (2011).

[31] M. Anselmino, V. Barone and A. Kotzinian, Phys. Lett. B **713**, 317 (2012).

[32] C.C. Chang et al. Phys.Rev.D27 (1983) 1983.

[33] D. Sivers, Phys.Rev.D79 (2009) 085008; see also arXiv:0910.5420

[34] A. Bacchetta, U. D'Alesio, M. Diehl and C. A. Miller, Phys. Rev. D **70** (2004) 117504 [arXiv:hep-ph/0410050].

[35] A. Kotzinian, private communication.

[36] L. Trentadue and G. Veneziano, Phys. Lett. **B 323**, 201 (1994).

[37] http://www.jlab.org/conferences/DIS2011/

[38] http://www.jlab.org/∼avakian/tmp/clasDIS-2010.january.tar.gz

[39] T. Sjostrand, arXiv:hep-ph/9508391.

[40] P. Astier *et al.*, [NOMAD Collaboration], Nucl. Phys. **B588** (2000) 3;
D. V. Naumov [NOMAD Collaboration], AIP Conf. Proc. **570** (2001) 489, hep-ph/0101325.

[41] V. Ammosov et al, *Nucl. Phys.* **B162**, 208 (1980).

[42] S. Willocq et al, (WA59 Collaboration), *Z. Phys.* **C53**, 207 (1992).

[43] M. R. Adams *et al.* [E665 Collaboration], Eur. Phys. J. **C17**, 263 (2000), hep-ex/9911004.

[44] A. Airapetian *et al.* [HERMES Collaboration], Phys. Rev. **B64**, 112005 (2001); Phys. Rev. **D 74** 072004 (2006); arXiv:0704.3133.

[45] M. Alekseev *et al.* [COMPASS Collaboration], Eur. Phys. J. **C 64** 171 (2009).